15th International Conference on Cold Regions Engineering, Quebec, Canada, August 19-22, 2012

Benchmarks for Solving Coupled Thermal, Hydraulic, and Air (THA) Numerical Models in Roadways in Cold Regions

Murray Fredlund, Jim Zhang
SoilVision Systems Ltd, Saskatoon ,SK , Canada

ABSTRACT: The cold climate environment can cause damage to engineering structures such as roadway/railways and pipelines. There has been an increased use of finite element numerical models to study and understand the processes involved. The primary difficulty in the application of such numerical models is the lack of proper coupling between the related processes of water, thermal, and airflow. This paper presents classic benchmarks solved with a finite element numerical modeling code which demonstrates the correct coupling of the thermal, hydraulic, and air (THA) processes. The use of this technology potentially opens the use of numerical models to a wider range of applications in artic regions.

KEY WORDS: soil freezing/thawing, natural convection, air/water/heat coupling flow, Elder problem, numerical model, density-dependent flow, heat transfer.

1 INTRODUCTION

With the economic development and ever increasing demand in energy resources, engineering activity in Polar Regions is increasing. The design of roadways, railways, and pipelines can be affected by thermal and water/air flow processes and their interaction with permafrost. The cold climate environment can cause damage to engineering structures such as roadway/railways and pipelines. Chen et al (2008) addressed many innovative technologies in order to protect the permafrost roadbed in the design of the Qinghai-Tiebet Railway, for example, using natural convection of air or thermosyphons etc. to cool embankments. Natural convection of air is a coupled process of air density-dependent flow and convective heat transfer. On the other hand, the process of oil density-dependent flow and convective heat transfer cannot be neglected in the analysis of oil leak propagation in the soil.

Elder (1967) presented a significant experiment and numerical analysis on the buoyant process created by a water case heated from below. There has since been an increased use of finite

element numerical models to study and understand the processes involved. Goring et al (1999, 2003), Jiang et al (2004), Sun et al (2007), and Lebeau and Konrad (2009) represent some of the subsequent studies. This paper presents of numerical modeling of the coupling of the thermal, hydraulic, and air (THA) processes by using the SVHeat, SVFlux, and SVAirFlow softeare (SoilVision System Ltd) in the following engineering applications.

2 BECHMARK 1: UNCOUPLED HEAT CONVECTION WITH STEADY-STATE WATER FLOW (ERH 1971)

Erh et al. (1971) presented experiments and an analytical solution to the heat convection problem under a constant water flow. The SVHeat software is utilized for the analysis of this model which contains the process of thermal conduction and convection with a constant water flow.

2.1 Model description

The schematic of the model configuration is illustrated in Figure 1. The water flows at a constant rate, v, from the bottom to the top of the cylindrical soil column. The temperature of flowing water, T_w, is applied on the lower end of the soil column, and the temperature at the upper end of the soil column is equal to ambient temperature, T_{amb}. The thermal flux on the lateral surface of the cylindrical soil column is calculated based on the thermal convection coefficient, h_c. To simulate the water flow velocity effect on the heat convective transfer, 10 models wre created.

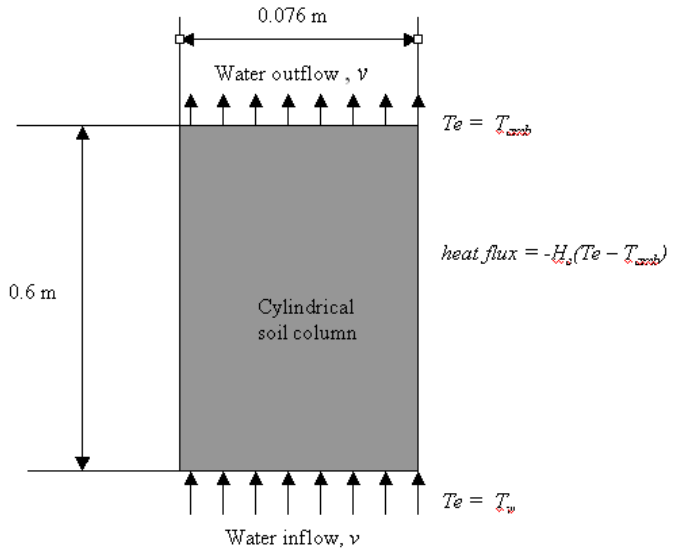

Figure 1: Model geometry of Erh convection problem with steady-state water flow

It is worth noting that the height of soil column is extended from 0.3 *m* to 0.6 *m* to approximate the boundary condition of $T = T_{amb}$ when $z = \infty$ in original Erh's analytical solution. However, only the temperatures from the elevation of 0 to 0.3 *m* are recorded in the simulation. No initial condition is required for the steady-state problem in this benchmark.

2.2 Material Properties

The material properties are illustrated in Table 1. Soil freezing and thawing are not considered in the benchmark.

Table 1 Material properties in Erh problem

Material name	Material properties	Symbols	Value	Units

Hanford sandy loam	Thermal conductivity	λ	1.47	J/s-m-oc
	Thermal convection coefficient	hc	10.4657	J/s-m2-oC
Aiken clay	Thermal conductivity	λ	1.47	J/s-m-oc
	Water thermal expansion	hc	10.4657	J/s-m2-oC

2.3 Results and Discussion

The dimensionless temperature *T1* and elevation *Z1* were employed in the analytic solution (Erh, 1971), and they are defined as follows:

$$T1 = (T - T_{amb})/(T_w - T_{amb}) \quad [1]$$

$$Z1 = z/L \quad [2]$$

where: T_1 is the dimensionless temperature; Z_1 is the dimensionless elevation; T is the soil temperature in ^oC; T_{amb} is the ambient temperature in ^oC; T_w is the temperature of water inflow in ^oC, and L is a reference length , L = 0.03 *m*.

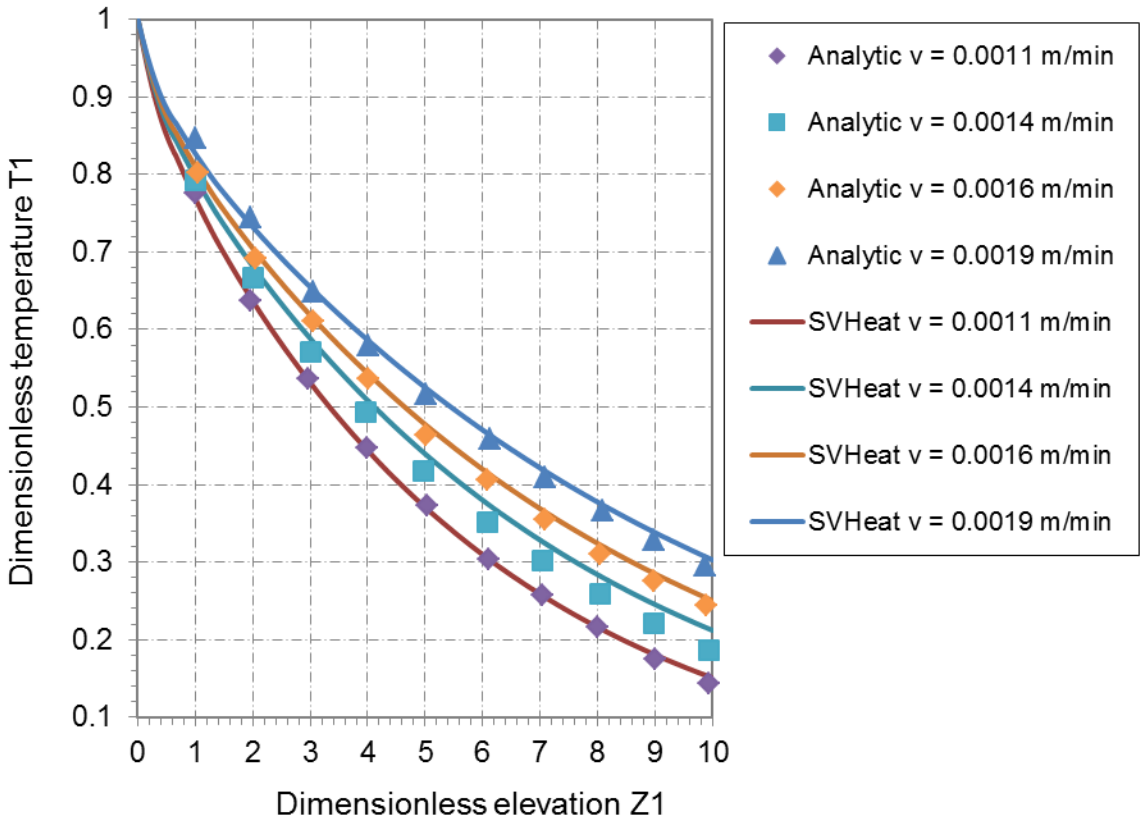

Figure 2: Comparison of the SVHeat simulation with the analytic result (Erh et al., 1971) for an Aiken clay in the case where interflow water temperature = 10 ^oC,

Figure 2 is the result simulated with SVHeat compared to the analytical result presented by Erh et al (1971), in which the temperature and elevation are represented with a dimensionless value as defined in equation [1] and [2]. Figure 3 is the comparison of the simulation with experimental results for Hanford sandy loam. It can be seen from both figures that the simulation agrees with the analytical and experimental result well.

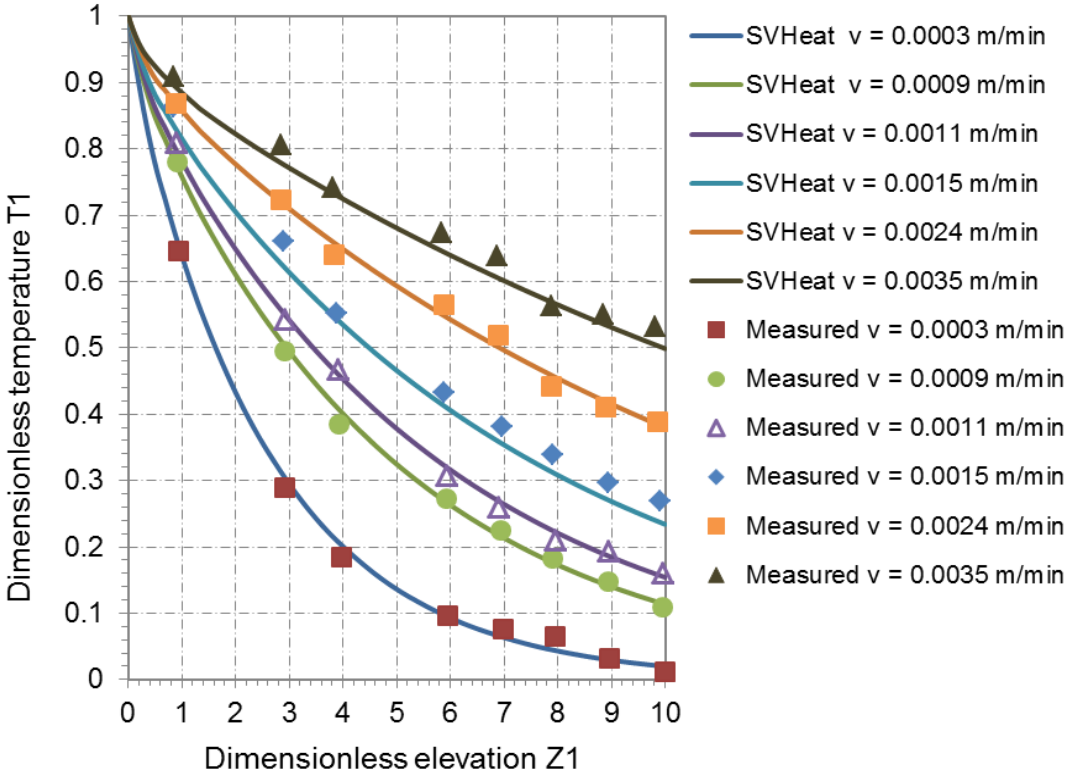

Figure 3: Comparison of SVHeat simulation with the experimental result (Erh et al., 1971) for Hanford sandy loam in the case of inflow water temperature = 30 ^{o}C

3 BENCHMARK 2: ELDER PROBLEM - COUPLED WATER AND HEAT FLOW WITH CONVECTION AND DENSITY-DEPENDENT FLOW (ELDER 1976)

Elder (1976) presented a numerical analysis of convective heat flow. The analysis has since been regarded as a standard benchmark of buoyant convection. This benchmark uses the coupled model of water and heat flow including the effect of water convective flow and density dependent flow due to the thermal expansion of water to simulate buoyant convection. The problem has been set up using the commercially available SVHeat and SVFlux software.

3.1 Model Description

The model is made up of rectangular geometry with a length of 600 *m*, and a height of 150 *m* (see Figure 4). The continuous heating source is applied along the segment of the model bottom. At the top of the model domain, the temperature is maintained at 0 ^{0}C. Other sides are thermally insulated. At the top-left corner B-E and top-right corner F-C, a constant value of water head, *h* =

0 *m*, is maintained. No water flow is allowed on any of the other sides of the model domain. The initial water head = 150 *m*, and initial temperature: 0 ^{o}C.

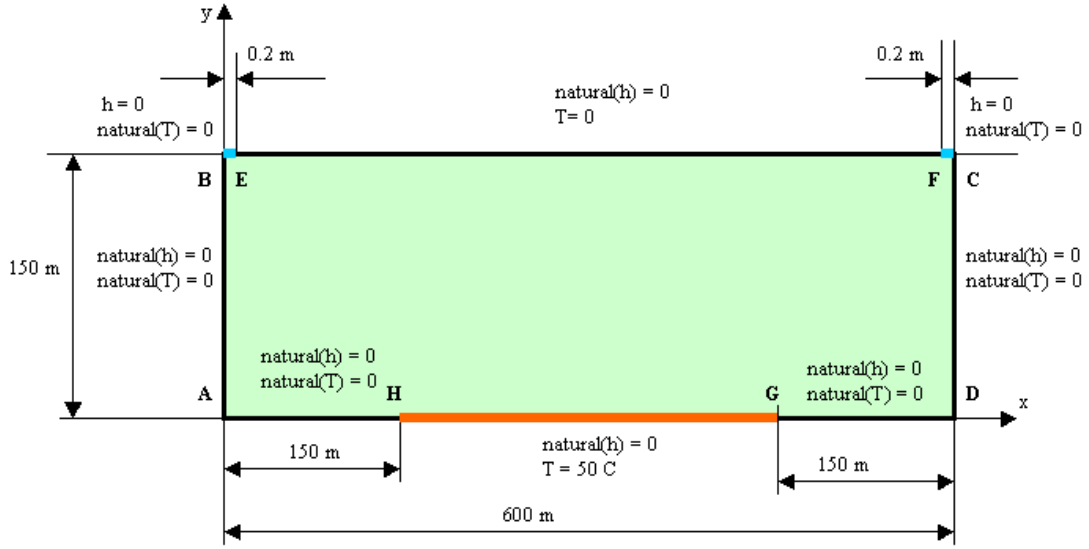

Figure 4: Model geometry of Elder convection heated below

3.2 Material Properties

The material of the model is saturated, and soil freezing and thawing are not considered in the model. The material properties are illustrated in Table 2.

Table 2 Material properties for Elders hot water rising problem

Material properties	**Symbols**	**value**	**units**
Sat hydraulic conductivity	Ksat	4.75295E-06	m/s
Saturated water content	satVWC	0.1	m^3/m^3
Thermal conductivity	λ	1.52	$W/m\text{-}^{o}c$
Soil heat capacity	*C*	418700	$J/m^3\text{-}^{o}C$
Water heat capacity	*Cw*	4187000	$J/m^3\text{-}^{o}C$
Water thermal expansion	betaT	4.07E-3	$1/^{o}C$

It is noted that the above material properties together with model configuration settings are required to meet the Rayleigh number, *Ra* = 400, that is used for the Elder problem.

3.3 Discussion of Results

The temperature patterns simulated with SVHeat and SVFlux are shown in Figure 5. The simulation time is set to 10 years. The pattern of temperature distribution for the Elder problem is sensitive to the mesh spacing. Figure 6 illustrates the effect of different mesh spacing on the symmetry of the contours, indicating that when the mesh spacing is less than 3 *m*, the distribution of temperature trends to be symmetric.

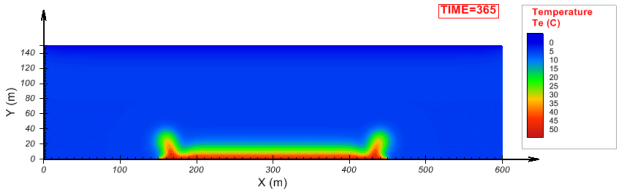

a. Temperature pattern after the 1st year

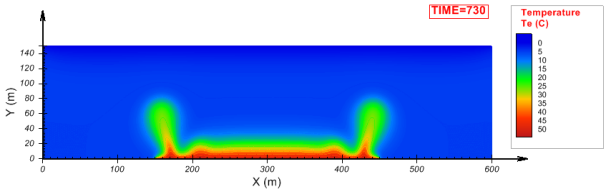

b. Temperature pattern after the 2nd year

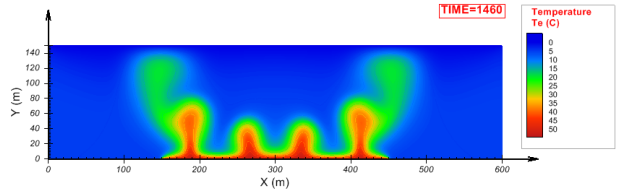

c. Temperature pattern after the 4th year

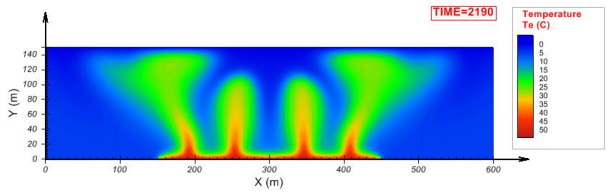

d. Temperature pattern after the 6th year

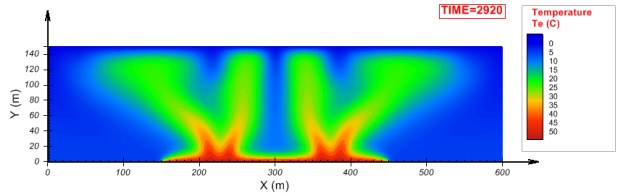

e. Temperature pattern after the 8th year

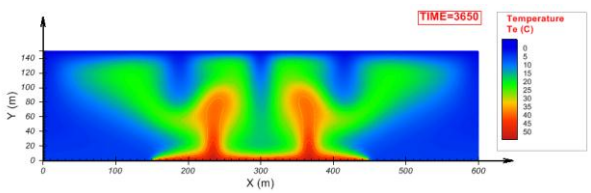

f. Temperature pattern after the 10th year

Figure 5: Temperature patterns of Elder convection problem simulated with SVHeat and SVFlux

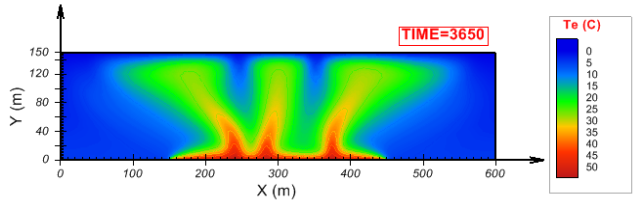

a. Implicit mesh spacing, nodes = 4787

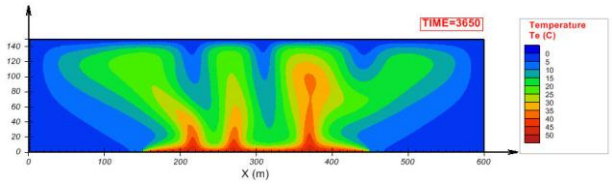

b. Mesh spacing = 5 m, nodes = 17250

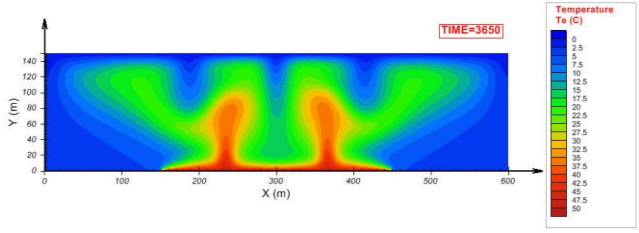

c. Mesh spacing = 3 m, nodes = 45383

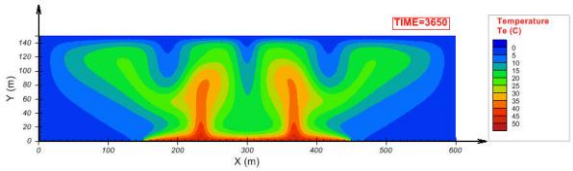

d. Mesh pacing = 2 m, nodes = 99606

Figure 6: Mesh spacing effect on the contour symmetry of Elder problem

4 BENCHMARK 3: CONVECTIVE COOLING EMBANKMENT (GOERING 2003)

Goering (2003), Sun et al (2007), and Lebeau (2009) have conducted a numerical simulation of cooling an embankment using natural convection. The intent is to protect railway or roadway

construction from thawing in permafrost areas. This example presents the characteristics of air buoyant flow and temperature distribution as governed by natural convection within the embankment using the SVAirFlow and SVHeat software.

4.1 Model description

The model geometry of the right half of a symmetric roadway is shown in Figure 7. The embankment is constructed with ballast type of material that has high air permeability. The pore-air in the embankment is allowed to approach equilibrium with the surrounding atmosphere. The climate temperature changes with time, as described in equation [3]. The ground foundation is assumed to be uniform silt material with high water content. On the natural ground surface, the air transfer on the boundary is assumed to be impermeable, and the climate temperature varies with time by equation [3]. The air is assumed to be incompressible in natural convection.

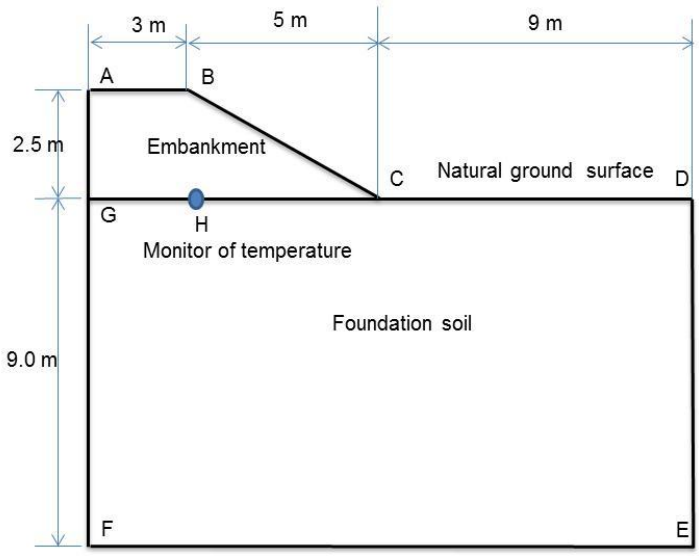

Figure 7: Model geometry for air convection cooling embankment

4.2 Boundary conditions

Goering (2003) presented the empirical equation [3] and equation [4] to describe the climate temperature change at the embankment surface (AB and CD), and ground surface BC. The air pressure that is applied to the surface AB and CD is calculated using the equation [5] according to the climate temperature of Equation [6]. A geothermal flux with the value of 0.06 w/m^2 is applied at the boundary of foundation bottom. The initial conditions are set to a temperature = 2 ^oC, and the initial pore (gauge) air pressure u_a = 0 *kPa*.

$$T_{abc} = 1.1 - 26.1\cos\left(\frac{2\pi}{365}(t-9)\right) \quad [3]$$

$$T_{cd} = -1.9 - 10.0\cos\left(\frac{2\pi}{365}(t-9)\right) \quad [4]$$

$$u_{abc} = gy\rho_0\left(1 - \beta(T_{amb} - T_0)\right) \quad [5]$$

$$T_{amb} = -3.8 - 20.0\cos\left(\frac{2\pi}{365}(t-9)\right) \quad [6]$$

where T_{abc} is the temperature applied to the embankment surface *ABC* in ^oC; T_{cd} is the temperature applied the natural ground surface *CD* in ^oC; T_{amb} is the ambient temperature in ^{o}C; u_{abc} is the air

pressure on the surface ABC in *kPa*; ρ_0 is the air density at a reference temperature in kg/m^3; *g* is the gravitational acceleration in m/s^2; β is the air expansion coefficient in $1/^0$C, and $\beta = 1/(237.15 + T_a)$; T_a is the pore air temperature in ^0C; T_0 is a reference temperature of 20 ^0C; *t* is time in *day*; and *y* is elevation relative to the ground surface in *m*.

4.3 Material Properties

The main properties of material used in the model are based on the values from Goering, as shown in Table 3.

Table 3 Material properties used in the convective air-flow model

Material	Porosity	Thermal conductivity ($w/m\text{-}^oC$)	Heat capacity ($J/m^3\text{-}^oC$)	SFCC	Air Intrinsic conductivity (m^2)
Embankment	0.35	0.346	1.020E+6	None	6.3E-7
Natural ground	0.45	Calculated by Johansen method: quartz content = 25%	unfrozen soil: 3750000 frozen soil: 2380000	Multi-linear estimation	1.0E-10

The air conductivity of a material in airflow is calculated based on air intrinsic permeability and air dynamic viscosity that is a function of air temperature. The thermal conductivity of heat transfer is calculated using the Johansen approach for the given quartz content. Please see SVAirFlow and SVHeat Theory Manual for a detailed description on how the theoretical formulation makes use of the material properties.

4.4 Result and Discussion

The model is simulated for 21 years to eliminate the effect of the initial condition on the temperature in ground foundation. The following briefly discusses and compares the results with other software.

4.4.1 The patterns of convective air flow in the embankment

During winter, the cool air at the embankment surface enters into the embankment. This happens because the air density increases with the decrease in temperature. The warm air then flows out from the lower region in the embankment to the atmosphere by the process of natural convection, as illustrated in Figure 8. The onset of natural convection occurs between October and November. After that time the amount of convective airflow increases with the decrease in temperature until March. The convective flow reduces with the increase in temperature after the end of March (see Figure 8). During the summer, because the temperature on the embankment surface is higher than the temperature at the lower region in the embankment, a small amount of convective airflow occurs in the embankment.

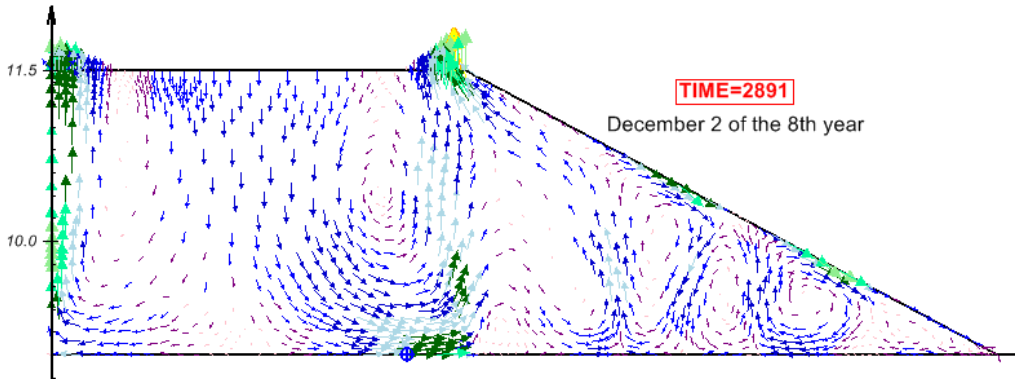

a: Mean air velocity = 4.98 m/s

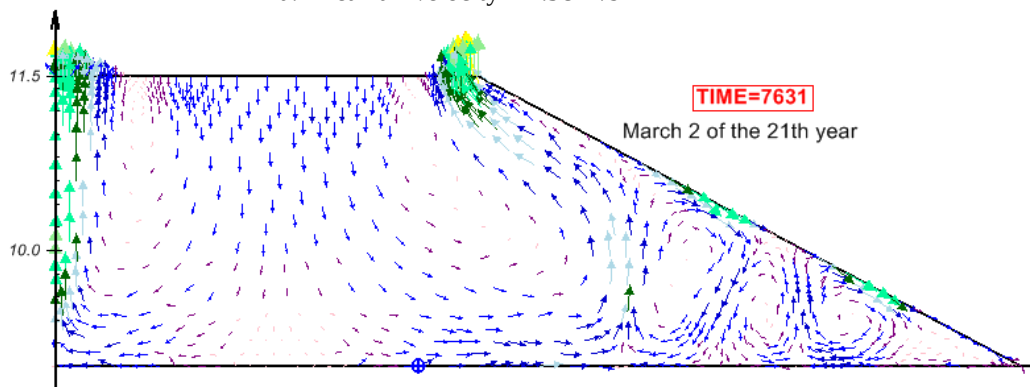

b: Mean air velocity = 6.24 m/s

Figure 8 Patterns of air convective airflow in the embankment

As illustrated in Figure 8, multi-airflow loops are formed in wintertime. For the two neighboring convective airflow loops, if one flows clockwise, another must move anti-clockwise. This characteristic of natural convection was also discussed in other research (Chen et al., 2008). Goering has simulated the results similar to Figure 8. It should be noted that the exact comparison to the flow vectors is not possible as Goering did not publish enough specifics of the modeling process.

Figure 9 further illustrates the comparison of the average value of airflow velocity at various locations with the value obtained by Goering. It should be noted that the airflow velocity for Goering in Figure 9 is the average value of airflow velocity magnitude over the whole embankment. This may be why the airflow velocity simulated in this benchmark in the SVAirFlow software has greater variation than Goering's value.

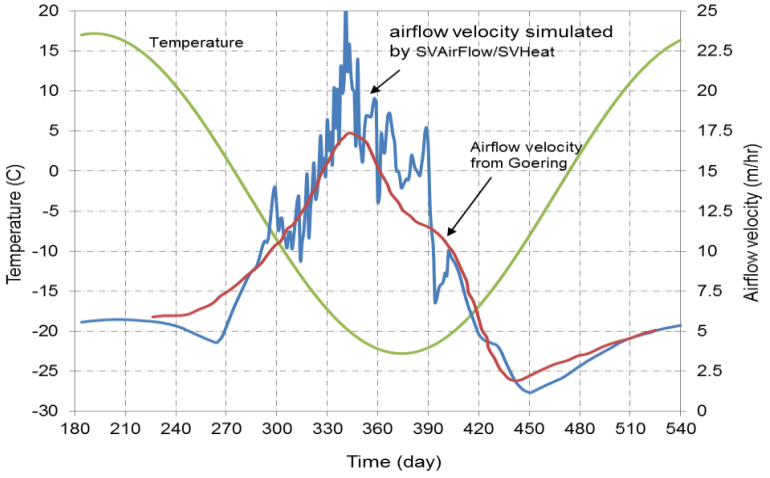

Figure 9: Comparison of airflow velocity in the embankment

4.4.2 Temperature distributions with nature convection

The maximum soil temperature at the ground base of the embankment is of particular interest to evaluate the embankment stability in the permafrost area. The construction of a railway or highway in the permafrost area was built above the permafrost layer. If the soil temperature below the ground surface of the embankment is above the soil freezing point, the thaw settlement of permafrost results in damage to the embankment.

Figure 10 shows the changing cycle of soil temperature with time at the base of embankment. It can be seen that the maximum soil temperature during the summer at the ground base of embankment changes from the initial value of 2 ^{o}C to 0 ^{o}C after about 9 years. This implies the embankment base is cooling due to the effect of natural convection.

Figure 11 illustrates the temperature contours on October 3 after a simulation time of 20 years. It can be seen from this figure that the temperature contour at the base of embankment is close to 0 ^{o}C.

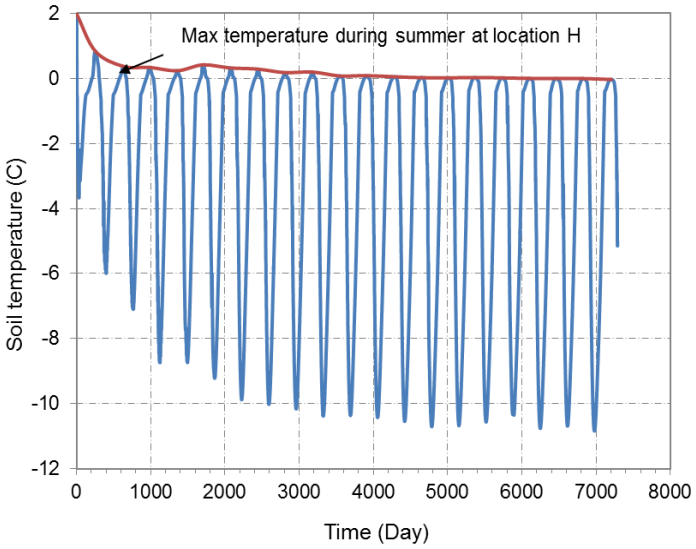

Figure 10: Soil temperature changing with time at the base of embankment

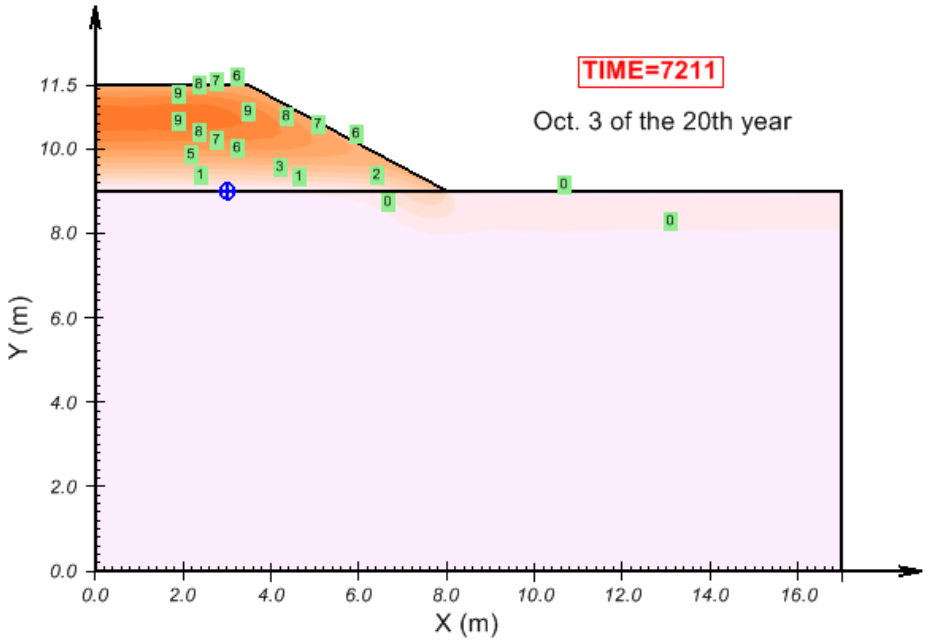

Figure 11: Temperature contour within the embankment on October 3 after 20 years

5 CONCLUSIONS

This paper has presented numerical analysis of the coupled model of water, air, and heat flow using the commercially available SVFlux, SVAirFlow, and SVHeat software to solve engineering problems with the processes of the water density-dependent or air density-dependent flow and convective thermal transfer. SVFlux, SVAirFlow, and SVHeat can be employed to simulate the triple coupling process of water-air-heat flow. The benchmarks are successful and demonstrate a close comparison between the software and published results. As a further future study, the snow influence and subsequent cooling effect of the embankment can also be simulated by applying a snow climate boundary.

REFERENCES

Chen, G. Wu, Q. and Ma, W. (2008). *Innovative Designs of Permafrost Roadbed for the Qinghai-Tibet Railway*. Science in China Series E: Technologic Sciences, 52(2): 530-538.

Elder, J.W. (1967). Transient Convection in a Porous Medium. J. Fluid Mechanics, 27: 609-623.

Goering, D.J. (2003). *Passively Cooled Railway Embankments for Use in Permafrost Areas*. J. Cold Regions Engineering. 17(3): 119-133.

Goering, D.J. and Kumar, P. (1999). *Permeability Effect on Winter-Time Natural Convection in Gravel Embankment*. Advances in Cold-Region Thermal Engineering and Science. 533: 455-464.

Jiang, F. Lie, S., Wang H., and Chen H. (2004). *The Air Flow and Heat Transfer in Gravel Embankment in Permafrost Areas*. Science in China Ser D Earth Science, 47: 142-151.

Lebeau, M., Konrad, J-M. (2009). *Natural Convection of compressible and incompressible gases in undeformable porous media cold climate conditions.* Computers and Geotechhics, 36: 435 – 445.

Nield, D. A, and Bejan, A. (2006). *Convection in Porous Media*, Third Edition, Springer-Verlag, New York.

Sun, B. Yang, L., and Xu, X. (2007). *Onset and Evaluation on Winter-time Natural Convection Cooling Effectiveness of Crushed-Rock Highway Embankment*. Cold Regions Science and Technology, 48: 218 – 231.